31st Congress of the International Council of the Aeronautical Sciences

Belo Horizonte, Brazil; September 09-14, 2018

INVESTIGATION ON APPROACH TO CONTROL LIFT DISTRIBUTION OF WING BY DISTRIBUTED PROPELLERS

Xue Chen* , **Zhou Zhou*** , **Wang Hongbo***

***School of Aeronautics, Northwestern Polytechnical University, Xi'an, 710072, PR.China**

Keywords: *Distributed propeller, asynchronous propeller, LEAPTech, BEM, vortex method*

Abstract

In this paper, the lift distribution of the wing after distributed propeller is studied. Using a high efficient hybrid fast calculation method (BVP), we can calculate a lot of different states to analyze the influence of distributed propeller on the wing lift distribution.

It can be seen that there are many factors which can affect the wing load distribution. In this paper, it is found that the position of the propeller, the rotation speed and the rotation direction have great influence on the lift distribution, while the chord direction and the vertical position have little influence on the shape of the spread lift distribution. The calculation results also show that when the propeller number increases, the total power demand is reduced. However, this paper does not match the propeller and the wing properly, so it can not show the further potential of the distributed propeller.

1 Nomenclature

C_L	=	lift coefficient of wing
C_{D_p}	=	press drag coefficient of wing
T_{single}	=	thrust of single propeller
P_{single}	=	power of single propeller
P_{total}	=	total power of all propellers
ΔZ	=	vertical position/m
ΔX	=	position of downstream flow/m
ΔY	=	span position/m

2 Introduction

Leading Edge Asynchronous Propellers Technology (LEAPTech)[1, 2, 3, 4] shows great potential in many aspects, such as, blowing the wing during takeoff and landing; also could be used to change the surface lift distribution of the wing and so on. It is useful to change the wing lift distribution, which can provide a solution to the problem of flexible wing deformation. But how to change it?

Because of the limitation of computational resources and time, most of the current research is focused on synchronous propellers' aerodynamic performance, and not very concerned about the changes in lift distribution on wing. Therefore, the purpose of this paper is to investigate the effects of the asynchronous propeller on the lift distribution of the wing by a rapid method.

3 Numerical methods

The RANS method is used to simulate the interaction between propeller and airfoil with high accuracy, and more flow field information can also be obtained. However, the object of this paper is the interference between the distributed propellers and wing. Using the RANS method to calculate the individual rotating components consumes a lot of computing time, not to mention the multi-propeller layout studied in this paper, so we must adopt a more efficient calculation method.The panel method can simulate the disturbance of propeller and wing. But for multi propeller layout, the panel method is used to cal-

culate the propeller,there will be a lot of helical wake element need to be calculated, which makes the calculation efficiency decrease, although the calculation takes less time than RANS, but still is not conducive to the early design.For example, if the number of wings' elements is l, there are m propellers, and the number of the wakes' elements of each propeller is n, and the number of iterations becomes $l \cdot m \cdot n$ times. Obviously, for the multi-propeller layout of this paper, it is not suitable to adopt the panel method to calculate the propeller and the wing directly. Therefore, a more efficient hybrid method(BVP) is used in this paper: the wing is calculated by the Panel method, the propeller is calculated by the Blade Element Momentum theory(BEM), and the interference between the propeller and the wing is calculated by the Vortex theory, in which the vortex theory input is circulation which are obtained from the BEM. It avoids a lot of wake calculation, thus greatly improving the computational efficiency.

3.1 Methods

(1) Unsteady Panel Method

A first-order potential-based Panel Method is used to analyze the wing aerodynamics. Low-order methods are clearly faster and cheaper to operate, and more importantly, low-order elements are more accurate for the same run time[5]. What's more, in this paper, the model calculates the flight speed is low, in the incompressible state, low-order panel method is sufficient.

In order to solve the problem of unsteady motion, two coordinate systems are applied, one is fixed on the ground coordinate system (Inertial frame of reference), a coordinate system with the movement of the body (Body-fixed frame of reference) as shown in Fig.1.Therefore, boundary condition has to take into account the transformed velocity ν. and thus becomes:

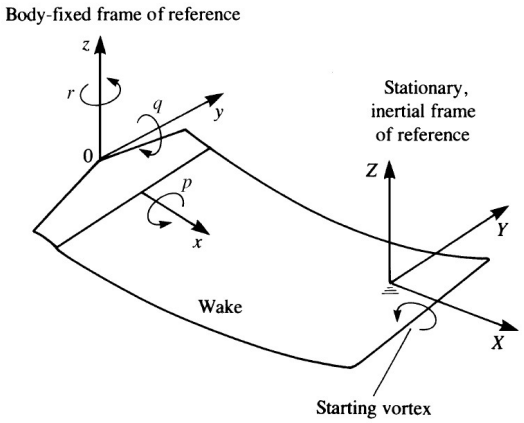

Fig. 1 : Coordinate system of unsteady panel method

$$(\nabla\Phi+\nu)\cdot\boldsymbol{n}=0 \quad \text{(in body fixed coordinates)} \tag{1}$$

Detailed calculation process can refer to bibliography[5].

(2) Blade Element Momentum Theory (BEM)

This paper uses an improved method based on the BEM for propeller aerodynamic characteristics calculation. The method used in this paper refers to the solution in bibliography [6]: a hypothesis is introduced, assuming that the resultant velocity induced by the propeller at the disk is perpendicular to the actual velocity of the blade element, the calculation results show that this assumption does not result in more errors, but also improves the computational robustness and computational efficiency. The detailed equation can be found in bibliography[7].

(3) Vortex Theory

Vortex Theory is used to estimate the velocity field induced by propeller in this paper. Just like a wing can be modelled by an appropriate combination of vortex lines or vortex sheet (Lifting-Line or Lifting-Surface Theory), the propeller can be represented by a series of helicoidal vortex

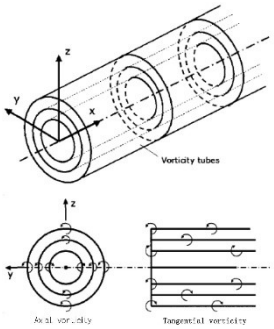

Fig. 2 : Coordinate system of unsteady panel method

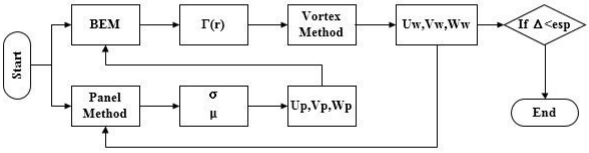

Fig. 3 : Coordinate system of unsteady panel method

sheets. The calculation of the velocity field induced by the helicoidal vortex sheet model of the slipstream is quit complex. A simpler model[8] has been modelled to estimate the overall induced effects in this paper. In this model, the helicoidal vortex sheets are replaced by two continuous distributions of vorticity, the axial vorticity and the tangential vorticity, as shown in Fig.2.

The detailed equation can be found in bibliography[8]. The specific calculation shows that the effect of the disk on the rear is very small, and the induced speed is 10^{-16} orders of magnitude, so it is neglected in this paper.

4 Propeller/Wing Interaction Calculation Method

In this paper, it is believed that the interference between the propeller and the wing is achieved by the induced velocity .The flow chart of algorithm is shown in Fig.3.

In the Fig.3, $\boldsymbol{\sigma}$, $\boldsymbol{\mu}$ represent source strength and doublet strength, respectively; U_p, V_p, W_p represent the blade elements' velocity induced by wing in three direction, respectively; U_w, V_w, W_w represent the surface elements' velocity induced by propeller in three direction, respectively.

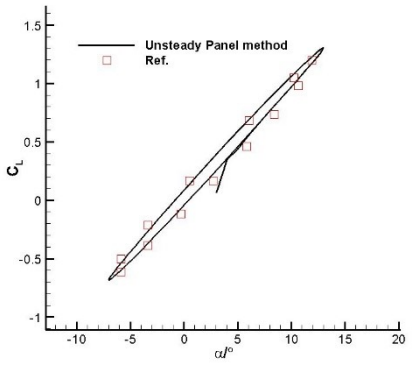

Fig. 4 : Lift loop for pitch oscillation of a wing with NACA0012 airfoil

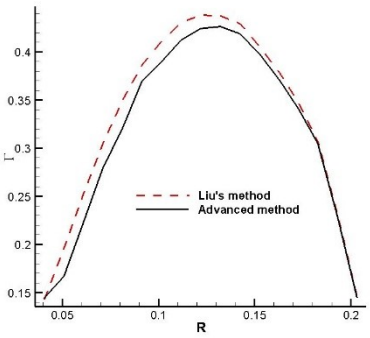

Fig. 5 : Thrust and power comparison between the calculation and the experimental value

5 Validation

(1) Wing performance

A three dimensional rectangular wing with an aspect ratio of 10 (airfoil: NACA0012) is used in this paper. A large-amplitude pitch oscillation of the wing has been calculated as shown in Fig.4 with Ref[9].

(2) Propeller performance

16×8propeller model is used to verify the reliability of the program. The free-stream

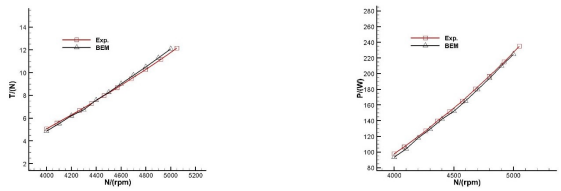

(a) Thrust (b) Power

Fig. 6 : Thrust and power comparison between calculation and experimental

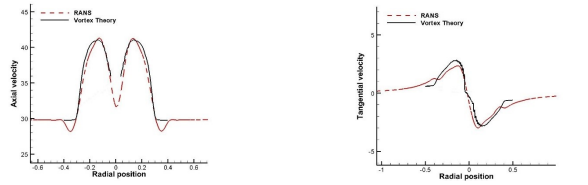

(a) Axial velocity (b) Tangential velocity

Fig. 7 : Comparison of axial and tangential velocity

velocity is 13m/s. Fig.5 shows that difference between the improved method and Liu's method.

(3) Velocity behind propeller

Another propeller model, which the free-stream velocity is 30m/s is used in this section. Fig.7a shows the comparison of the axial and tangential velocities calculated by the vortex theory with RANS simulation.

6 Results and analysis

In this paper, the key factors such as the number of propeller, the position of the installation, the rotating speed and the rorating direction of the propeller were studied. The rotation direction of the propeller is defined in this paper: observed from the rear of the wing, clockwise rotation is '-'. The counter clockwise rotation is '+'.

6.1 Influence of number of propeller

When the aircraft is in flight, the thrust and drag balance needs to be ensured. In this case, the required thrust can be provided by a small number of propellers, so that each propeller needs to provide a larger thrust. Of course, multiple propellers may also provide the required thrust, at this time, each propeller only need to provide smaller thrust, so what kind of state is more beneficial to the flight? In order to ensure that the variable is single, each configuration produces the same total thrust when considering the effect of the quantity in this parper. In this paper, 4, 6, 8 and 10 propellers are calculated respectively. The detailed state is shown in Table 1

Table 1: Propeller status in each case

	Number of propeller	T_{single}/N	P_{single}/W
case1	4	10.45	199.2
case2	6	6.67	124.8
case3	8	5.01	94.6
case4	10	4.01	77.1

Table 2: Calculation results of case1-case4

	C_L	C_{D_p}	P_{total}/W
case0	0.171	0.0204	-
case1	0.180	0.0242	796.8
case2	0.190	0.0239	748.5
case3	0.187	0.0233	756.5
case4	0.186	0.0229	770.9

The total thrust of the four cases is about 40N. The calculated results are as follows:

From the results in the Table 2, it can be seen that increasing the number of propellers reduces the total power requirement and the lift does not decrease when the number of propellers is within a certain amount, which means that the distributed propeller can achieve the purpose of reducing the energy consumption of flight. But it can be seen from the table that, when the number of propellers continues to be increased, the power will gradually increase. It also means that as the propeller layout increases with the number of propellers, the propeller size needs to be smaller, which may result in less energy consumption.

The distribution of the lift in these four cases is shown in the Fig.8.

It can be seen that the propeller obviously changed the span-wise lift distribution of the

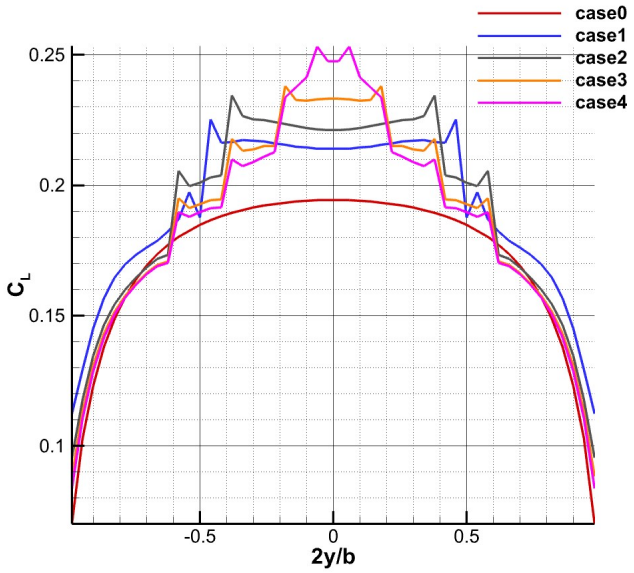

Fig. 8 : Spanwise lift distribution of case1-case4

wing. In case1-case4, the lift in the lift distribution near the root of the wing showed a pit in the lift due to the axial acceleration and upwash of the propeller is not obvious in this area, making the lift drop.

6.2 Influence of spanwise position

For aircraft with large aspect ratio, the spanning dimension is very large relative to the chord direction. Therefore, there are many possibilities for the propeller's mounting position. How can the installation get the most benefit? This section has been studied in this section, which is also carried out under the premise that the total thrust is about 40N.

Case5-case8: the propeller installation position moved to the wingtip corresponding tocase1-case4, while case9-case12 moved to the wing root, respectively.

It can be seen from the calculation results that when the propeller moves toward the wingtip, more lift augmentation will be obtained. On the contrary, the lift to the root of the wing will reduce the lift augmentation. Of course, this is related to the direction of rotation of the propeller, where the propellers rotate toward the wingtip (left wing propeller '+', right wing propeller '-'). This can be more clearly understood from the

Table 3: Lifting coefficient and pressure drag coefficient for different spanwise positions

Number of propeller	case	C_L	C_{D_p}
4	case1	0.180	0.0242
	case5	0.196	0.0252
	case9	0.183	0.0218
6	case2	0.190	0.0239
	case6	0.197	0.0250
	case10	0.184	0.0219
8	case3	0.187	0.0233
	case7	0.196	0.0247
	case11	0.184	0.0214
10	case4	0.186	0.0229
	case8	0.198	0.0244
	case12	0.183	0.0216

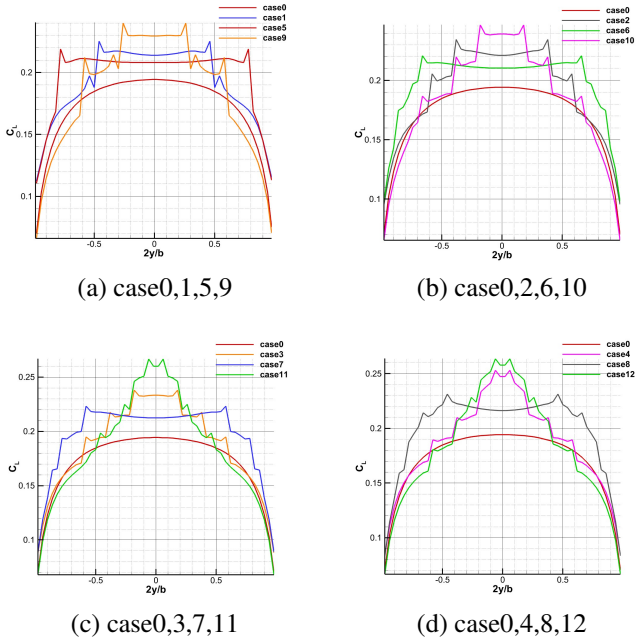

(a) case0,1,5,9 (b) case0,2,6,10

(c) case0,3,7,11 (d) case0,4,8,12

Fig. 9 : Lift distribution of different spanwise position

Table 4: Lift coefficient and pressure drag coefficient for different ΔY in two proprllers

	ΔY	Rpm	C_L	C_{D_p}
case0	-	-	0.171	0.0204
case13	0.5	3600	0.176	0.0212
case20		4800	0.175	0.0209
case14	1	3600	0.174	0.0205
case21		4800	0.173	0.0205
case15	2	3600	0.171	0.0204
case22		4800	0.176	0.0209
case16	4	3600	0.171	0.0205
case23		4800	0.177	0.0211
case17	6	3600	0.172	0.0206
case24		4800	0.179	0.0214
case18	8	3600	0.173	0.0207
case25		4800	0.182	0.0220
case19	10	3600	0.174	0.0212
case26		4800	0.185	0.0236

following: case13-case19(case20-case26) are the two propellers with 3600rpm(480rpm) gradually move to the wingtip:

As can be seen from Table4 and Fig.10, as the propeller moves toward the wingtip, the lift gradually increases. And from Fig. 11, when the propeller's position moves outward, the upwash area of the propeller increases. Meanwhile, the influence of the propeller's down wash is also decreasing, which together leads to the larger lift. Of course, from Fig.10, it can be seen that when the propeller is close, the lift appears relatively large. This may be due to the mutual influence of the propellers here, which may be a numerical problem and needs further verification.

6.3 Influence of vertical position

This section makes a simple study of the vertical position of the propeller installation, which is carried out in the case of the total thrust about 40N.

As can be seen from Table5 and Fig.12, for any number of propeller configurations, when the vertical position of the propeller is moved forward along the Z axis, the lift will gradually increase. It can be seen from the figure, when

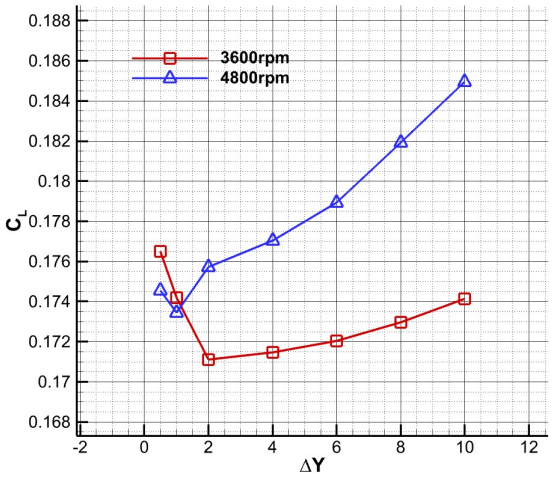

Fig. 10 : The lift coefficient at different ΔY values

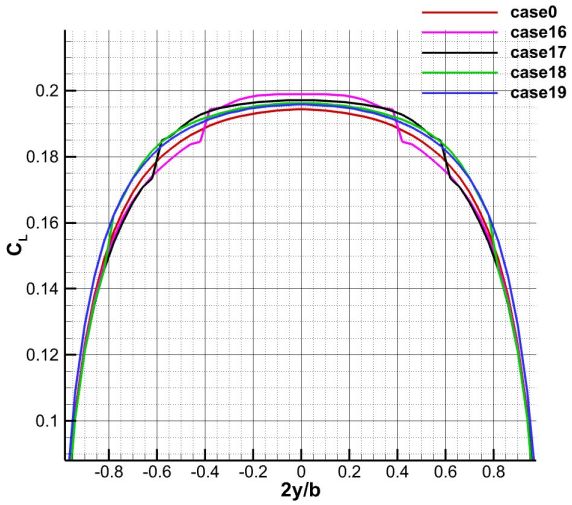

Fig. 11 : Spanwise lift distribution of case16-case19

Table 5: Lift coefficient and pressure drag coefficient for different ΔZ in two proprllers

Number of propeller	ΔZ	case	C_L	C_{D_p}
4	0	case1	0.180	0.0242
	0.05	case27	0.187	0.0212
	0.10	case31	0.188	0.0244
	0.15	case35	0.190	0.0214
	0.20	case39	0.180	0.0220
	0.25	case43	0.177	0.0220
6	0	case2	0.190	0.0239
	0.05	case28	0.191	0.0244
	0.10	case32	0.194	0.0244
	0.15	case36	0.195	0.0235
	0.20	case40	0.179	0.0220
	0.25	case44	0.177	0.0218
8	0	case3	0.187	0.0233
	0.05	case29	0.188	0.0240
	0.10	case33	0.193	0.0241
	0.15	case37	0.196	0.0231
	0.20	case41	0.178	0.0213
	0.25	case45	0.176	0.0216
10	0	case4	0.186	0.0229
	0.05	case30	0.184	0.0233
	0.10	case34	0.190	0.0238
	0.15	case38	0.194	0.0229
	0.20	case42	0.178	0.0212
	0.25	case46	0.175	0.0215

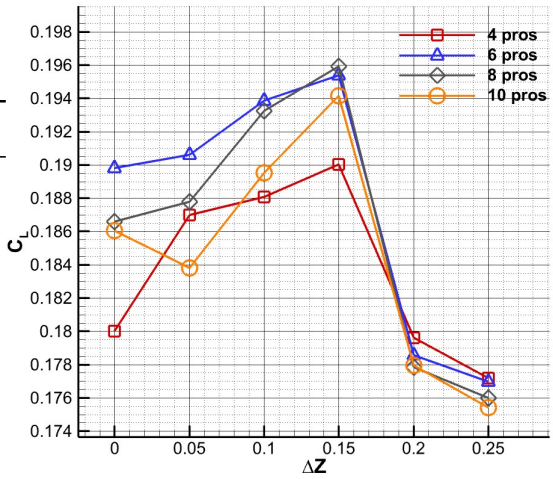

Fig. 12 : The lift coefficient varies with ΔZ

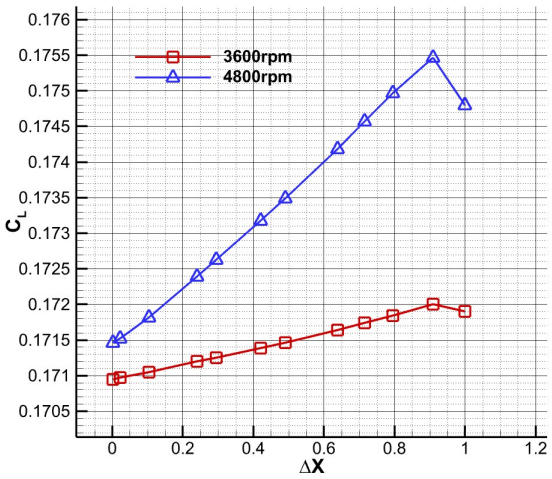

Fig. 13 : The lift coefficient varies with ΔX

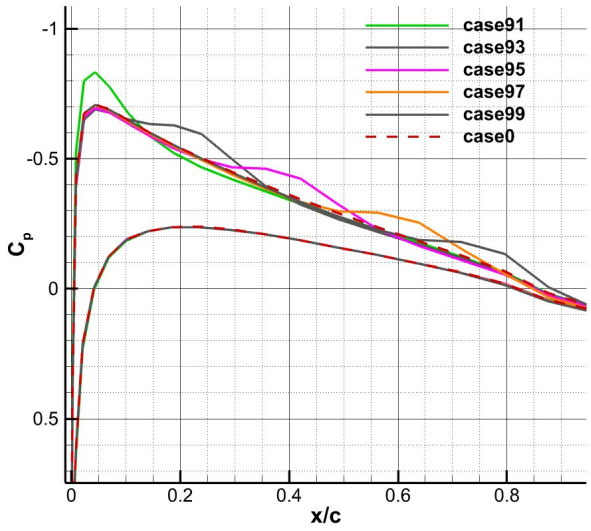

Fig. 14 : Wing pressure distribution with different propeller chord positions

the Z/R=0.75, the lift reached the maximum, and then with the vertical position to continue upward, the lift will slowly fall. This is mainly because the vertical position changes, changed the proportion of diversion in the upper and lower wing surface of propeller slipstream, with the vertical position of the large slip flow on the surface of the wing on the accelerating effect more obvious, and the maximum thrust of propeller is about 70%, so when the Z/R= 0.75, the acceleration effect of propeller slipstream most significantly, the lift becomes larger. With the further increase of the vertical position, the propeller slipstream deviated from the upper surface of the base, the accelerating effect of slipstream is not obvious, the lift will become smaller.

6.4 Influence of chordwise position

The impact of the propeller chord-mounted position on wing was studied in this section. In order to ensure comparability of results, the distance between the propeller and the wing at each chordwise position is 0.05c. The result is as follows:

As can be seen from Fig.13, as the chord position moves towards the trailing edge of the wing gradually, the lift of the wing first increases slowly. When the position reaches ΔX/c = 0.9,

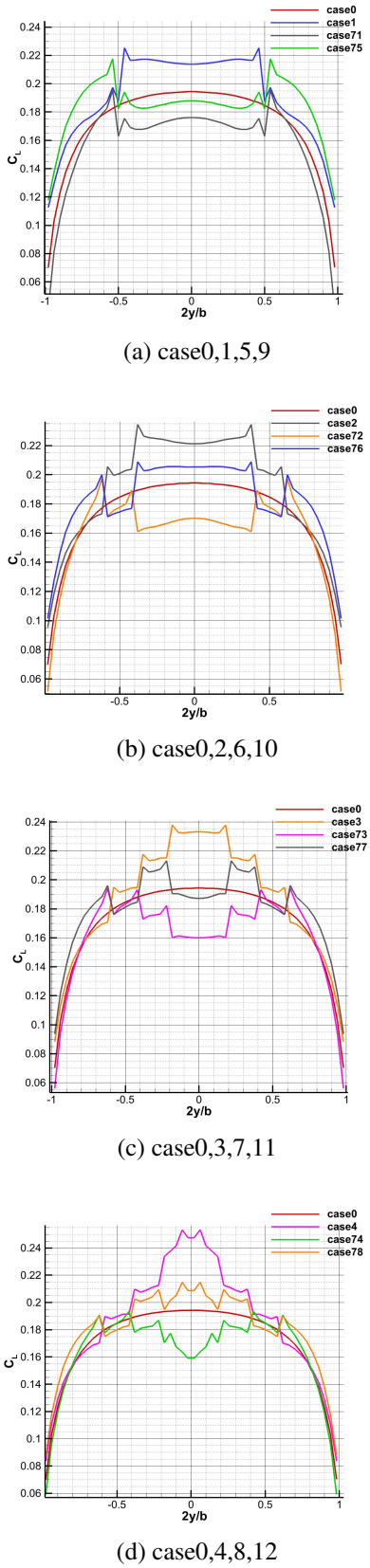

(a) case0,1,5,9

(b) case0,2,6,10

(c) case0,3,7,11

(d) case0,4,8,12

Fig. 15 : Lift distribution of different spanwise position

the lift reaches the maximum, and then the lift begins decline. This is mainly because the propeller is installed above the upper surface of the wing at this time, and the wing acts as a blocking effect on the slipstream of the propeller. Propeller washings and washings are not as pronounced as they were before. At this time, the leading role is the suction effect of the paddle, and as the chord of the propeller moves backward, the influence of the propeller suction and jet action on the wing gradually becomes larger and the lift force becomes larger. However, when the position continued backward, propeller wake acceleration began to weaken, lift began to decline.

It can be seen from the pressure distribution in Fig.14 that the pressure distribution on the lower surface is basically unchanged compared with the case without a propeller, and the influence of the propeller is mainly concentrated on the upper surface of the wing. In addition, it can be seen that the suction near the propeller disk is obvious and the pressure on the upper surface near the disk is significantly reduced because of the acceleration of the air flow caused by suction.

6.5 Influence of rorating direction and speed

After a given propeller, the flow field behind the propeller is entirely determined by the rotation direction and speed of the propeller itself, so it is necessary to study the two factors correspondingly. Similarly, to make sure that the total thrust unchanged under the circumstances of this part of the study. Change the case of case1-case4 to case71-case74 (left wing propeller '-', right wing propeller '+') and case75-case78 (counterrorating).

From Table6, it can be seen that the lift augmentation obtained when the propellers all rotate toward the wingtip (left wing propeller '+', right wing propeller '-') is the highest, whereas the lift augmentation obtained when the propellers all rotate toward the wing-root(left wing propelle '-', right wing propeller '+') is the smallest.

The fundamental reason is that the direction of rotation of the propeller changes the size of the upper washing zone and the downwashing zone of the wing. When the propeller rotates towards the wingtip, the upwash effect is greater than downwash and the lift force becomes larger. When the propeller turns into a counter-rotating mode, the propeller's interference will be more intense and the lift distribution will show more irregularities, as shown in Fig.15a.

This also means that there is a possibility of achieving the purpose of controlling the wing load by changing the direction of rotation of the propeller.

Table 6: Lift coefficient and pressure drag coefficient for different rorating direction

Number of propeller	case	C_L	C_{D_p}
4	case1	0.180	0.0242
	case71	0.157	0.0168
	case75	0.183	0.0232
6	case2	0.190	0.0239
	case72	0.159	0.0176
	case76	0.183	0.0229
8	case3	0.187	0.0233
	case73	0.162	0.0182
	case77	0.180	0.0223
10	case4	0.186	0.0229
	case74	0.164	0.0185
	case78	0.180	0.0220

7 Conclusions

(1) From the above results, it can be seen that there are many factors which can affect the wing load distribution. However, it is obvious that the installation position towards spanwise, rotation direction and speed of the propeller have the greatest impact on the wing load distribution, the chordwise and vertical positions only have a certain impact on the value of the lift, which do not fundamentally change the lift distribution towards wing spanwise;

(2) It can be seen from the calculation results in this paper that the propeller installed on the tip of the wing has a great influence on the aircraft. Therefore, it is considered

that install a larger propeller at the tip of the wing while the aircraft design stage, it may provide required lift only by these two propellers, of course, it is also good for reducing the cruise drag;

(3) From the calculation results of this paper, it is possible to attain the purpose of wing load control using distributed propeller. From the result, it can obtain a radically different spanwise lift distribution when changing the propeller rotation direction and speed , It can imagine that if the aircraft wing suffer from a upward sudden gust on the left side, the lift on the left wing becomes larger firstly and the airplane tends to roll to the right, which may bring about a series of troubles. At this time, if the propellers of the left wing change to rotate towards wing root, it may curb the lift increase of the left wing, that make the purpose of gust mitigation come true;

(4) This paper is only a preliminary exploration of the possibility of distributed propeller on the wing load control, and does not involve the design of propeller and wing, so some of the conclusions in this paper are not optimal, and did not fully dig out the biggest advantages of the distributed layout, author may pay attention to this point in the future research.

References

[1] Alex M Stoll. Comparison of cfd and experimental results of the leaptech distributed electric propulsion blown wing. In *15th AIAA aviation technology, integration, and operations conference*, page 3188, 2015.

[2] Alex M. Stoll, Joe Ben Bevirt, Mark D. Moore, William J. Fredericks, and Nicholas K. Borer. Drag reduction through distributed electric propulsion. In *Aiaa Aviation Technology, Integration, and Operations Conference*, 2014.

[3] Jeffrey K. Viken, Sally Viken, Karen A. Deere, and Melissa Carter. Design of the cruise and flap airfoil for the x-57 maxwell distributed electric propulsion aircraft. In *Aiaa Applied Aerodynamics Conference*, 2017.

[4] Michael D. Patterson and Brian German. Conceptual design of electric aircraft with distributed propellers: Multidisciplinary analysis needs and aerodynamic modeling development. In *Aerospace Sciences Meeting*, 2015.

[5] org.cambridge.ebooks.online.book.Author@e. *Low-Speed Aerodynamics*. Springer Netherlands, 2009.

[6] MIT. *Qprop theory document*. web.mit.edu.drela.Public.web.qprop.qproptheory.pdf, 2007.

[7] Peiqing Liu. *Theory and application of air propeller*. Beihang University press, 2006.

[8] L.L.M. Veldhuis. *Propeller Wing Aerodynamic Interference*. PhD thesis, Technische Universiteit Delft, 06 2005.

[9] W. J Mccroskey, K. W Mcalister, L. W Carr, and Pucci. Dynamic stall on advanced airfoil sections. *Journal of the American Helicopter Society*, 26(3), 1981.

Contact Author Email Address

Mail to: chenxue@mail.nwpu.edu.cn

Copyright Statement

The authors confirm that they, and their company or organization, hold copyright on all of the original material included in this paper. The authors also confirm that they have obtained permission, from the copyright holder of any third party material included in this paper, to publish it as part of their paper. The authors confirm that they give permission, or have obtained permission from the copyright holder of this paper, for the publication and distribution of this paper as part of the ICAS proceedings or as individual off-prints from the proceedings.